Supplementary Materials for

Rev-erbα Dynamically Modulates Chromatin Looping to Control Circadian Gene Transcription

Yong Hoon Kim, Sajid A. Marhon, Yuxiang Zhang, David J. Steger,

Kyoung-Jae Won*, and Mitchell A. Lazar*

*correspondence to:
wonk@pennmedicine.upenn.edu
lazar@pennmedicine.upenn.edu

This PDF file includes:

Materials and Methods

Animal studies

Male wild type C57/BL/6 mice (from JAX) were used in this study. The Nr1d1 (Rev-erbα) knockout mice were obtained from B. Vennström, and have been backcrossed to the C57BL/6 background for more than seven generations (*3*). All of the experiments were performed with male mice aged between 8-12 weeks. Mice were housed in a temperature-controlled, specific-pathogen free facility with a 12-12 light on-and-off cycle (light on at 7AM/ZT0 and off at 7PM/ZT12). All animal studies were carried out in concordance with an approved protocol from Institutional Animal Care and Use committee at Perelman School of Medicine at the University of Pennsylvania.

Gene transduction in mouse liver

Adeno-associated viruses encoding FLAG-tagged Rev-erbα or GFP under the liver-specific TBG promoter (AAV8-TBG-Rev-erbα-F, and AAV8-TBG-eGFP used as a negative control) were prepared by the Vector Core of the Penn Diabetes Research Center, as described previously (*6*). 5e11 virus particles were injected into each mouse by tail-vein injection, 2 weeks after which mice were harvested for analysis.

Isolation of hepatocyte nuclei

Mouse liver tissue (100mg) was dounced with 15 mL of cold swelling buffer (10mM HEPES, 2mM MgCl2, 3mM CaCl3) 10 times with piston A. After 20 min incubation on ice, the homogenate was dounced again 20 times with piston B, after which additional 15mL of cold swelling buffer was added. The homogenate was filtered through a 100mm cell strainer and spun at 400g in 4°C for 10 min. The supernatant was discarded, and the pellet resuspended in 10mL of cold swelling buffer containing 10% glycerol. 10mL of cold lysis buffer (swelling buffer + 10% glycerol +1% Igepal) was slowly added with occasional vortexing. After 5 min incubation on ice, 30mL of cold lysis buffer was added, after which it was spun down at 600g in 4°C for 5 min. The supernatant was discarded and the pellet resuspended with 25mL of cold lysis buffer and spun down at 600g at 4°C for 5 min again. The supernatant was discarded, and the pellet contained isolated, undisrupted nuclei. For ChIP and Hi-C experiments, these pure nuclei were crosslinked in 10 mL of PBS with 1% formaldehyde for 20 min at room temperature and quenched with 1/20 volume of 2.5M glycine solution for 5 min. The crosslinked nuclei were spun down at 600g at 4°C for 5 min, after which they were resuspended in Hi-C lysis buffer (10mM Tris-HCl pH8, 10mM NaCl, 0.2% Igepal) and spun down at 600g in 4°C for 5 min again. The supernatant was discarded, and crosslinked nuclei was used for ChIP and Hi-C.

Chromatin immunoprecipitation (ChIP).

ChIP experiments were carried out as previously described with a few changes (*3*). 1-5 million crosslinked nuclei were used per immunoprecipitation. Nuclear extract were prepared by sonication in lysis buffer (50mM Tris-HCl pH 8, 0.1% SDS, 10mM EDTA) using the Bioruptor (Diagenode) for a fragment range of 200-1000bp. Chromatin was immunoprecipitated in ChIP buffer (50mM Tris-HCl pH 7.5, 140mM NaCl, 1mM EDTA, 1% Triton X-100, 0.1% NaDOC) using 5-10ug of antibody, and reverse crosslinked overnight at 65°C in SDS buffer (50mM Tris-HCl, 10mM EDTA, 1% SDS,

pH 8). DNA was isolated using phenol/chloroform/isoamyl alcohol and second chloroform wash. Precipitated DNA was used for quantitative PCR or further processed for ChIP-seq. The antibodies and primers used for ChIP are listed in Table S1.

Quantitative PCR.

Quantitative PCR was performed with Power SYBR Green Mastermix and the PRISM 7500 instrument (Applied Biosystems). Analysis was carried out using the standard curve method. mRNA expression was normalized to the housekeeping *Rplp0* gene. Primer pairs used for ChIP-qPCR and RT-qPCR were listed in Table S1 and 2.

ChIP-seq

ChIP-seq was performed as described (*21*) with minor changes. Precipitated DNA was amplified by Phusion High-Fidelity DNA polymerase (NEB M0530) and processed according to the ChIP Sequencing Sample Preparation Guide by Ilumina. The following reagents were used: adaptor oligos and indexed primers from Illumina, all enzymes from New England Biolabs (NEB) and PCR purification and MinElute Kit from Qiagen. The Functional Genomics Core (J. Schug and K. Kaestner) at the University of Pennsylvania performed deep-sequencing using the Illumina HiSeq2000.

ChIP-seq data processing

ChIP-seq data were processed as previously described (*21*). The reads from biological replicates were pooled and aligned to the mm9 mouse genome. Browser tracks were processed by Homer v4.7 (*31*) and peaks were visualized on IGV (*33*). High confidence Rev-erbα peaks were identified by following parameters: two groups of peaks were called by FC 1.5> between ZT10 vs. ZT22 (physiological KO) and ZT10 vs. Rev-erbα KO (genetic KO). The overlapped peaks between these groups within 200bp were called as common peaks. The common peaks were further filtered by > 2rpm cutoff, yielding 2402 high confidence unique Rev-erbα peaks. ChIP-seq datasets are summarized in Table S3 and available in GEO (GSE104129).

GRO-seq data processing

GRO-seq data at ZT10 and ZT22 were downloaded (*6*) and gene body transcription level was calculated by counting reads beginning 500 bp downstream from the TSS in the strand where the gene is transcribed. Transcription tag counts were normalized by Reads Per Kilobase of transcript per Million (RPKM).

De novo motif analysis

De novo motif finding was performed by Homer v4.7 (*31*) . Motif discovery was performed with different motif lengths (8, 10, 12, 14,16, 18 and 20 bp). As the search for motifs longer than 15 bp was set in this analysis, a number of 4 mismatches has been allowed.

In situ Hi-C

In situ Hi-C was performed with mouse liver tissues using MboI restriction enzyme according to the protocol described (*14*) with minor changes. Instead of crosslinking cells directly, isolated and crosslinked hepatocyte nuclei were used. In addition, biotin from

unligated ends were removed by incubating 5ug of DNA in 50ul T4 DNA polymerase reaction (0.1ug/ul BSA, 1xNEB buffer 2, 25uM dGTP, 15U T4 DNA polymerase). The reaction was carried out at room temperature for 4 hours and stopped by the addition of 2ul of 0.5M EDTA pH 8.0 per 50ul reaction. Isolated Hi-C DNA was amplified by fewer than 8 PCR cycles to reduce PCR duplicates. Hi-C library were quantified by KAPA library preparation kit (Roche) and BioAnalyzer (Agilent). We note that, while genome organization in *Drosophila* is sensitive to temperature (*32*), Fig. S1B demonstrates reproducibility between the TAD boundaries we report in mouse liver and previously identified TAD boundaries in mouse embryonic stem cells (*7*) indicating that this technical issue likely does not have a major impact on our findings.

Chromatin conformation capture (3C)

3C experiments were carried out in the same manner as Hi-C except for minor changes. 10^7 isolated and crosslinked nuclei were used per each 3C experiment. HindIII enzyme was used instead of MboI. Biotin overhang fill-in step was omitted, and in-nuclei ligation was performed immediately after digestion with HindIII. After ligation, the supernatant was removed, the pellet containing nuclei resuspended in Hi-C lysis buffer and residual HindIII enzymes were denatured by incubating at 65°C for 30 min. The nuclei were spun down for 5 min at 600g, after which the supernatant was discarded, and the pellet containing nuclei was resuspended again in Hi-C lysis buffer. The nuclei were reversed crosslinked and treated with proteinase as stated in the Hi-C protocol. DNA was isolated using phenol/chloroform/isoamyl alcohol and second chloroform wash. Precipitated DNA was dissolved in water, and 100ng of DNA was used for each technical replicate for quantitative PCR with specific TaqMan probes. Standards were prepared using BAC (the CHORI BACPAC Resource Center) spanning an entire locus to be probed. HindIII digested and randomly ligated DNA fragments were diluted to 500ng/ml, 50ng/ml, 5ng/ml and used for 1000, 100, 10 arbitrary units for standard curves, respectively. All interactions are normalized to the intragenic interaction at the *TBP* locus to control for DNA amounts and crosslinking efficiency. The BAC, primers and probes used are listed in Table S5.

Hi-C data processing

Deep-sequencing of Hi-C libraries were performed by the Functional Genomics Core (J. Schug and K. Kaestner) at the University of Pennsylvania and the Penn Epigenetics/Cell and Developmental Biology Sequencing Core using the Illumina NextSeq 75 cycle (40bp paired-end sequencing). The sequences were processed using Hi-C Pro (*34*). Singleton and multi-hits reads were discarded. Each reported aligned pair was assigned a restriction fragment according the restriction fragment coordinates that have been created by digestion the genome using the MboI restriction enzyme. Invalid ligation products were discarded and only valid pairs with two different ligation fragments were kept to build the contact matrix after removing duplicated valid pairs. The built matrix included the inter- and intra-chromosomal interaction reads for the specified resolutions. The genome was split into bins of a specified size (5 kbps), and the reported valid pairs were associated to bins to form the interaction raw matrix of that bin size. We have created matrices of different bin sizes to be used in the analysis on the chromatin interaction. The raw matrices were normalized to correct for biases using the

ICE (Iterative correction of Hi-C data) (*35*) of Hi-C Pro. Hi-C library statistics are summarized in Table S4.

Differential Analysis

Differential analysis between interaction matrices of two Hi-C libraries was performed to highlight the difference between Hi-C interactions. We performed smoothing by applying 2D Gaussian filter (σ=2.0) using window size 17x17, followed by sharpening to detect and maintain edges of foreground regions. Background signals were masked for further processing. For differential analysis of a pixel, a surrounding 5x5 window was compared between the two matrices using t-test. If the p-value was significant, the center pixel of that window was considered significantly different.

Enhancer-promoter loop calling using Rev-erbα peaks

To detect the interaction between Rev-erbα peaks and the target genes, a 3x3 window was examined if at least 6 bins had an interaction greater than or equal to a particular loop cutoff threshold after ICE normalization. In this analysis, we used a loop cutoff of 10 (ICE normalized interaction value). If a loop included the promoter of a gene repressed at ZT10 (FC ≥1.5 ZT22 GRO-seq/ZT1 -GRO-seq), the Rev-erbα binding site was defined as "engaged"; otherwise, it was defined as "passive."

TAD and sub-TAD boundary calling

TAD calling was performed based on the directionality index (DI) method described previously (*7*). The TADs were called using the ICE Hi-C matrix with 40 Kbps bin size and with upstream and downstream directionality index bias within a 2 Mbps window. We also called the sub-TADs with different window sizes to detect hierarchical TADs (TADs and sub-TADs). We used window sizes 150 kbps, 250 Kbps, 500 Kbps, 1Mbp, and 2 Mbps in the analysis. We used bin size 10 kbps Hi-C interaction matrices in this hierarchical TADs calling.

Circadian sub-TAD analysis

Circadian sub-TADs have been defined as sub-TADs that include genes transcribed with a circadian rhythm (6). Circadian genes were grouped based on their phases (ZT0-3, ZT3-6, ZT6-9, ZT9-12, ZT12-15, ZT15-18, ZT18-21, and ZT21-24) (*6*). We used genes from the ZT9-12 and ZT21-24 groups to match the time points for the Hi-C libraries. For each sub-TAD, differential analysis was performed between ZT22 and ZT10 ICE-normalized Hi-C matrices, which resulted in ZT22-specific and ZT10- specific intra-sub-TAD interaction. The size-normalized sub-TADs were then averaged for each group of sub-TADs (ZT9-12-specific and ZT21-24-specific groups). The averaged sub-TADs of each group were converted into $\log_2$ scale for visualization.

TAD and sub-TAD boundary overlap

TAD overlap was determined by evaluating the conservation of TAD boundaries among ZT22, ZT10, and mESC Hi-C libraries. After calling TADs, the overlap between TAD boundaries of two or more different Hi-C libraries was performed by checking

locations of the 5’ end and 3’ end boundaries of the called TADs within a particular tolerance distance (200 kbps).

Figure S1

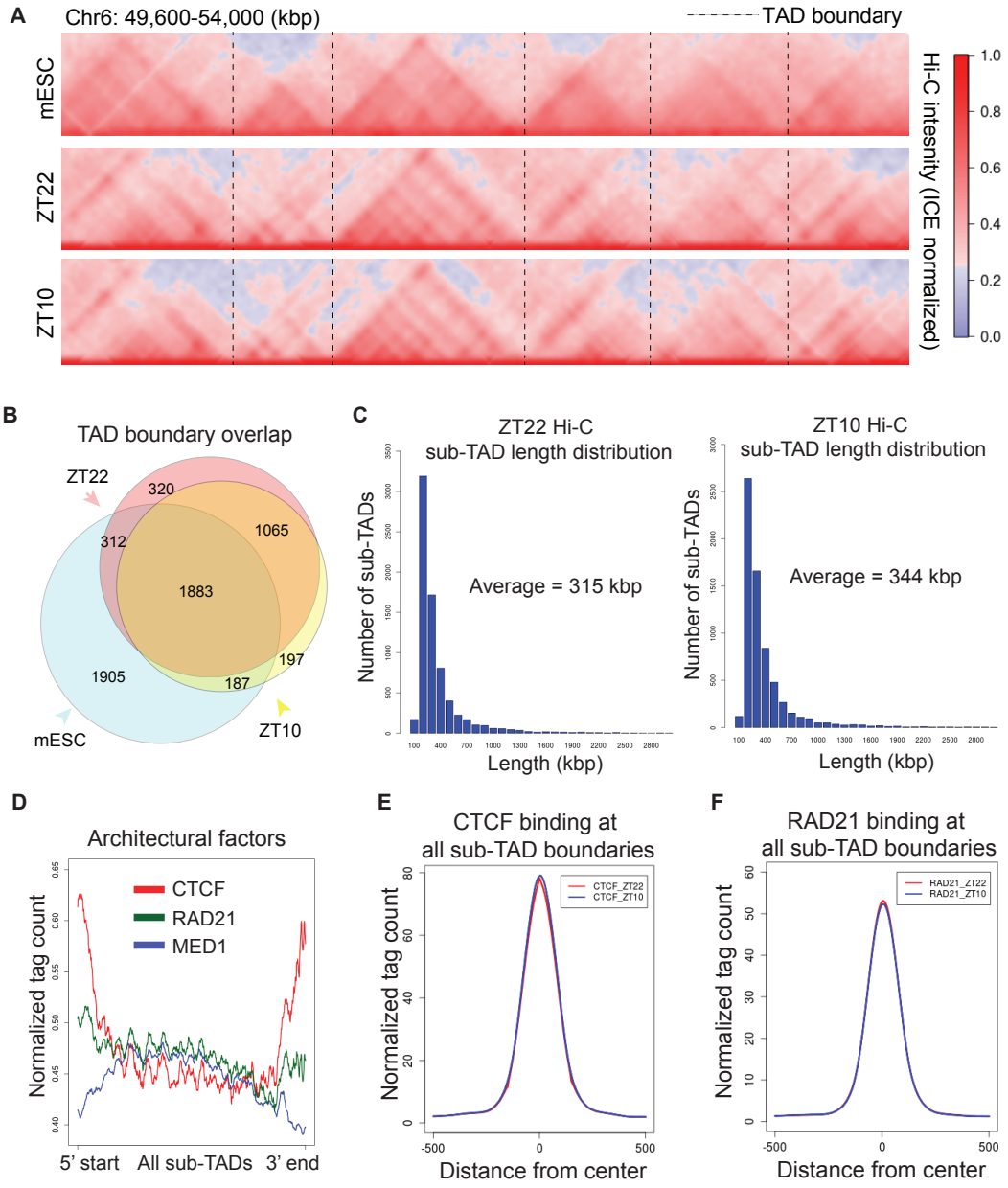

Fig. S1. Liver TADs and sub-TADs exhibit conserved boundaries and structure.

(A) Hi-C Heat maps of mouse embryonic stem cell (mESC), mouse liver at ZT22 and at ZT10 demonstrating conserved boundaries (dotted lines), represented as ICE-normalized Hi-C intensity. **(B)** Mouse ESC and mouse liver TADs demonstrated conserved boundaries genome-wide. **(C)** Size distribution of sub-TAD identified in ZT22 and ZT10 Hi-C, with average sizes of 315 kbp and 344 kbp, respectively. **(D)** Distributions of architectural factors CTCF (red), RAD21 (green), and MED1 (blue) within all sub-TAD size-normalized to standard 5' and 3' boundaries. **(E)** CTCF binding at ZT22 and ZT10 at the CTCF peaks identified within regions around sub-TAD boundaries (± 2kbp boundary). **(F)** RAD21 binding at ZT22 and ZT10 anchoring at the CTCF peaks identified in Fig. S1E.

Figure S2

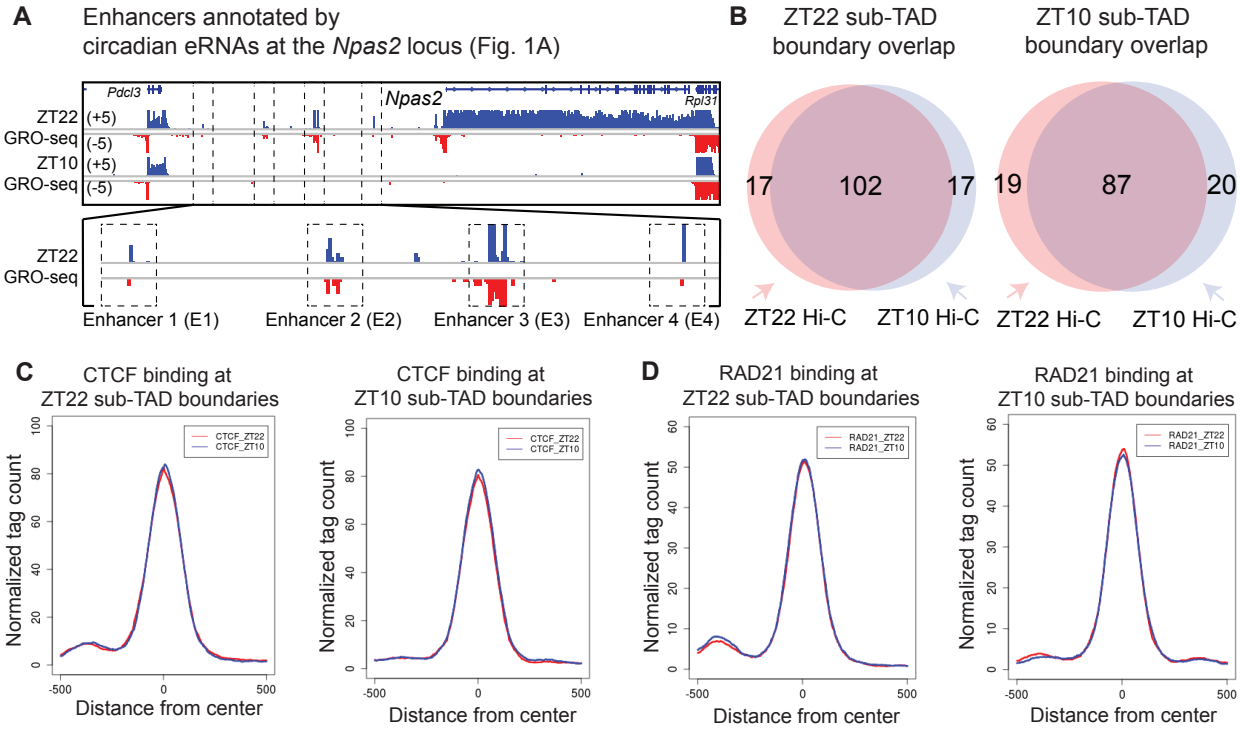

Fig. S2. Intra-TAD interactions are dynamically controlled within the boundaries of circadian sub-TADs.

(A) Enhancers annotated by divergent eRNA transcription (dotted box) upstream of the *Npas2* gene for Fig. 1A. **(B)** Boundary overlap of ZT22 and ZT10 sub-TADs in ZT22 Hi-C and ZT10 Hi-C. The boundaries for circadian sub-TADs are similarly identified in ZT22 Hi-C and ZT10 Hi-C. **(C)** CTCF binding at ZT22 and ZT10 at the CTCF peaks identified within regions around ZT22 (left) and ZT10 (right) sub-TAD boundaries (± 2kbp boundary). **(D)** RAD21 binding at ZT22 and ZT10 anchoring at the CTCF peaks identified in Fig. S2C.

Figure S3

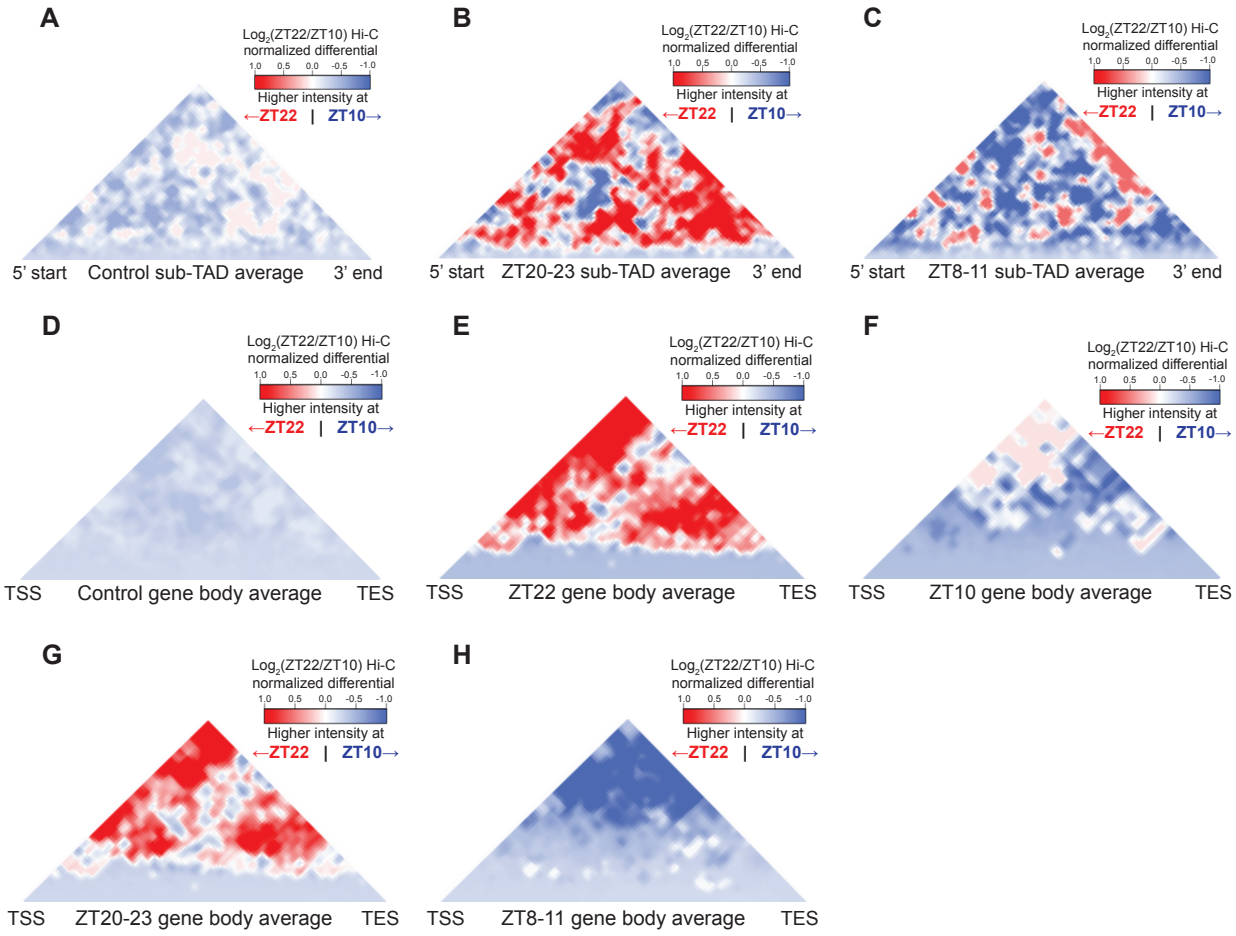

Fig. S3. Intra-TAD interactions and gene body contacts exhibit circadian rhythms.

(A) Averaged differential changes in intra-TAD interactions of 1800 non-circadian sub-TADs showed no appreciable difference. **(B)** ZT20-23 and **(C)** ZT8-11 circadian sub-TADs demonstrated averaged differential changes consistent with intra-TAD interactions. **(D)** Averaged differential changes in gene bodies for 2000 non-circadian genes. **(E)** ZT22 circadian genes, and **(F)** ZT10 circadian genes exhibited changes consistent with circadian intra-TAD interactions. **(G)** ZT20-23 and **(H)** ZT8-11 circadian genes also exhibited correspondingly consistent changes in gene bodies.

Figure S4

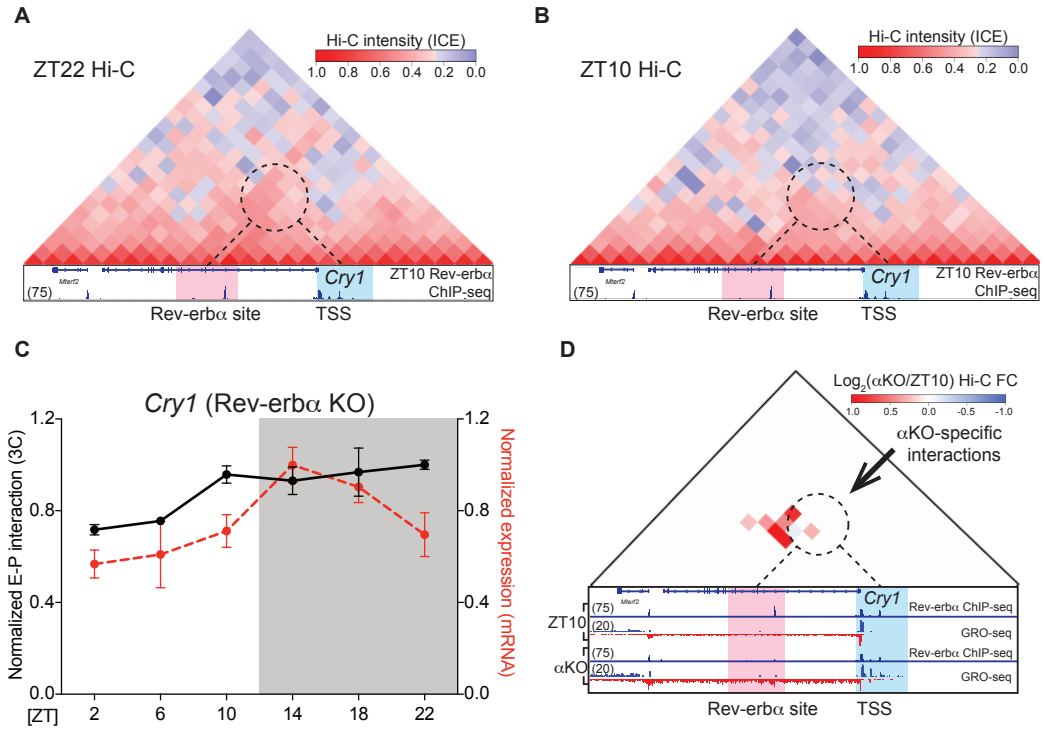

Fig. S4. Regulation of enhancer-promoter looping at the *Cry1* locus by Rev-erbα.

(A) ZT22 and **(B)** ZT10 Hi-C heat maps at the *Cry1* locus, represented as ICE-normalized Hi-C intensity. Stronger interactions were detected around Rev-erbα-regulated site (red) and TSS (blue) at ZT22 (dotted circle). **(C)** Circadian 3C with Rev-erbα KO livers exhibited attenuated rhythmicity consistent with mRNA expression (red dotted line). **(D)** Differential Hi-C analysis at the *Cry 1* locus revealing Rev-erbα KO (αKO)-specific interactions at ZT10, represented as $\log_2$ ratio (ZT10 Rev-erbα KO Hi-C/ ZT10 WT Hi-C). αKO-specific interactions (dotted circle) occur between a region around the intronic Rev-erbα site (red) and the *Cry1* TSS (blue). Global Run-On seq (GRO-seq) demonstrates increased nascent transcription in Rev-erbα KO at ZT10.

Figure S5

A

De novo motifs at engaged sites

PWM	Motif	p-value	%
	RORE	1e-39	33.04
	RevDR2	1e-21	18.26
	RXRA	1e-18	6.09
	HNF6	1e-15	33.91

B

De novo motifs at passive sites

PWM	Motif	p-value	%
	NR2F2	1e-59	61.40
	RXR	1e-33	21.76
	NF1-half	1e-20	35.23
	HNF4A	1e-19	30.83

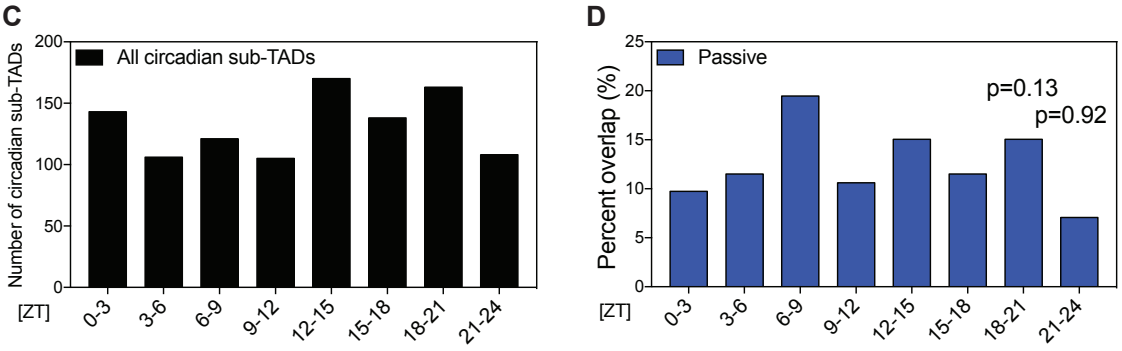

Fig. S5. Genomic characterization of Rev-erbα sites.

(A) De novo motif analysis at engaged Rev-erbα sites revealed enrichment of the known Rev-erbα DNA binding motifs. **(B)** De novo motif analysis at passive Rev-erbα sites did not show enrichment of such motifs. **(C)** The number of circadian sub-TADs from different phases showing a relatively even distribution. **(D)** Analysis of passive Rev-erbα sites with circadian sub-TADs did not show overlap with ZT18-24 circadian-sub-TADs.

Figure S6

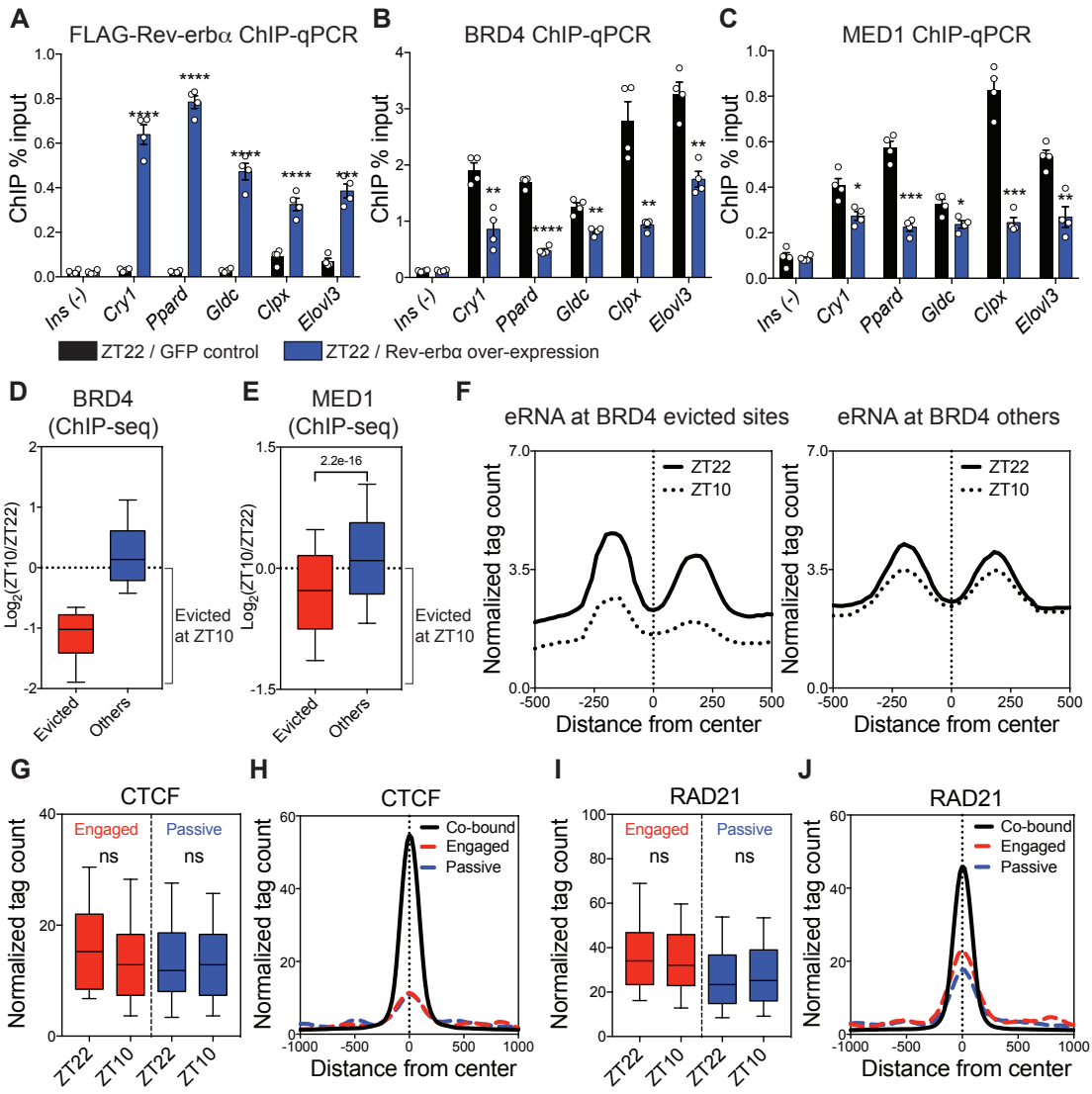

Fig. S6. Rev-erbα opposes recruitment of BRD4 and MED1, but not CTCF and RAD21.

(A) FLAG- Rev-erbα, **(B)** BRD4, and **(C)** MED1 ChIP-qPCR at engaged Rev-erbα sites upon ectopic expression of Rev-erbα at ZT22. **(D)** Rev-erbα sites sub-grouped into "BRD4-evicted" sites based on BRD4 binding fold changes ≥1.5 ZT22 ChIP-seq/ZT10 ChIP-seq. **(E)** BRD4-evicted Rev-erbα sites exhibit concurrent eviction of MED1 occupancy (Mann-Whitney tests). **(F)** BRD4-evicted Rev-erbα sites independently predict functional enhancers with circadian eRNA transcription. **(G)** CTCF binding at engaged and passive Rev-erbα sites at ZT22 versus ZT10. **(H)** Average profile of CTCF at CTCT-RAD21 co-occupied sites (black line), engaged (red), and passive (blue) demonstrated unappreciable binding of CTCF at Rev-erbα sites. **(I)** RAD21 binding at engaged and passive Rev-erbα sites at ZT22 versus ZT10. **(J)** Average profiled of RAD21 at CTCT-RAD21 co-occupied sites (black line), engaged (red), and passive (blue) also demonstrated unappreciable binding of RAD21 at Rev-erbα sites. For boxplots, whiskers drawn at 10^{th} and 90^{th} percentiles.

Table S1. ChIP reagents

ChIP antibodies

Protein	**Manufacturer**	**Catalog number**
Rev-erbα	Cell Signaling	2124
CTCF	Millipore	07-729
RAD21	Abcam	ab992
MED1	Bethyl	A300-793A
BRD4	Bethyl	A301-985A100

ChIP-qPCR primers

Site	**5' Forward**	**3' Reverse**
Ins	GGACCCACAAGTGGAACAAC	GTGCAGCACTGA TCCACAA T
Cry1	TTCCTTATGCCACTTCCAAAA	ATGCTAAACCACCCACTGGT
Ppard	CAAATGGGAAGCAGCGAGTA	CCAGCTGCCCTATCAATCAG
Gldc	GGTGGCCTCAAAATACACAGA	GTGGAGACAACTCCTGCACA
Cplx	TCTACCTCTCCTACCCCAAGG	AGCCTGTTTCACAGGAAGGA
Elovl3	TCACAAAAGGTACAGAGCCAAA	CAGCCAGTTAATATCTCCCATTG

Table S2. mRNA expression qPCR reagent

mRNA qPCR primers

Gene	**5' Forward**	**3' Reverse**
Rplp0	TCCAGGCTTTGGGCA TCA	CTTTATCAGCTGCACATCACTCAGA
Cry1	AGCGCAGGTGTCGGTTATGAGC	ATAGACGCAGCGGATGGTGTCG

Table S3. ChIP-seq library summary

Protein	Time	Replicates
CTCF	ZT22	2
CTCF	ZT10	2
RAD21	ZT22	2
RAD21	ZT10	2
MED1	ZT22	1
MED1	ZT10	1
MED1	ZT10 αKO	1
BRD4	ZT22	1
BRD4	ZT10	1
BRD4	ZT10 αKO	1
Rev-erbα	ZT22	2
Rev-erbα	ZT10	2
Rev-erbα	ZT10 αKO	2

Table S4. Hi-C library summary

ZT22 Hi-C unique valid read pair distribution	
valid_interaction	670515102
trans_interaction_all	265634607
cis_interaction_all	404880495
cis_shortRange (<20kbp)	151469116
cis_longRange (>20kbp)	253411379
Biological replicates	5

ZT10 Hi-C Unique valid read pair distribution	
valid_interaction	660903704
trans_interaction_all	247967408
cis_interaction_all	412936296
cis_shortRange (<20kbp)	185241695
cis_longRange (>20kbp)	227694601
Biological replicates =	2

αKO Hi-C Unique valid read pair distribution	
valid_interaction	539690196
trans_interaction_all	225494937
cis_interaction_all	314195259
cis_shortRange (<20kbp)	120205453
cis_longRange (>20kbp)	193989806
Biological replicates =	3

Table S5. 3C reagents

Bacterial artificial chromosome for *Cry1*
RP23-381A6

Cry1 probe sequence (5'-3')
GGATGTGCCGGCAAGTTGGT

Cry1 locus primers

Primer	**Sequence (5'-3')**	**Note**
Cry1_constant_F	AGCTCTTTTTGTTCCGCTCA	Constant primer
Cry1_1R	CCCATTCCTCTCCTTGTTCC	
Cry1_2R	GCTCTGAAACCACTTGCTCA	
Cry1_3R	CATGGAAGCTGTTAATTTCACTTG	
Cry1_4R	TCGGCAGCTTTTTACACTGA	Used for E-P loop
Cry1_5R	GTCGCAGGACCTCAAATTCA	
Cry1_6R	AATGCCCCTTGTCTGCATTA	
Cry1_7R	CACAGGGCAAGCCTTTCTT	
Cry1_8R	CAAAGTCTGAGCCCAGTCAC	

TBP probe sequences (5'-3')
TGGCTCCTCCCCTTTGAGATTTG

TBP primers

Primer	**Sequence (5'-3')**
TBP_constant_F	CATCTACTGAGAACATGATGAGGA
TBP_1R	CCCAAATAGTGTTGTCTGCAA

Supplementary references

31. S. Heinz *et al.*, Simple Combinations of Lineage-Determining Transcription Factors Prime cis-Regulatory Elements Required for Macrophage and B Cell Identities. *Mol. Cell*. **38**, 576–589 (2010).

32. L. Li *et al.*, Widespread Rearrangement of 3D Chromatin Organization Underlies Polycomb-Mediated Stress- Induced Silencing. *Mol. Cell*. **58**, 216–231 (2015).

33. J. T. Robinson *et al.*, Integrative genomics viewer. *Nat. Methods*. **29**, 24–26 (2011).

34. N. Servant *et al.*, HiC-Pro: an optimized and flexible pipeline for Hi-C data processing. *Genome Biol.* **16**, 259 (2015).

35. M. Imakaev *et al.*, Iterative correction of Hi-C data reveals hallmarks of chromosome organization. *Nat. Methods*. **9**, 999–1003 (2012).